Nr 5 ISSN 1509-5878 5/2011
AUTOBUSY
Technika, Eksploatacja, Systemy Transportowe

Przemysław BARTOSIK, Leon KUKIEŁKA

THREE DIMENSIONAL MODELING AND NUMERICAL SIMULATIONS OF SHOT PEENING PROCESS OF ENGINE PARTS

Abstract

Computer modeling and numerical simulation of shot peening process were the aim of this work. The mixed explicit-implicit method of plastic stress determination was proposed and presented. Incremental Lagrange formalism and adequate measures of strains and stresses were used in the paper. The physical, mathematical and numerical models of shot peening process were presented. The surface layer of object was treated as an elastic/viscous-plastic body with nonlinear mixed hardening. Although the shot was considered as ideally rigid or elastic body. The examples of numerical simulations were presented.

INTRODUCTION

Dynamic development of automotive industry enforces the manufacturers to use of advanced technologies, which provide simultaneously high structural strength, low production cost, and low mass of manufactured parts and components. One of technologies which allows to obtain those opposing requirements is shot peening process. It improves the mechanical properties of machine parts through modification of object surface layer properties. The surface layer state has a significant impact on the functional properties of machine parts. Therefore it is very important to know the patterns of all components of internal stress. Most of empirical research methods allows only to investigate the patterns of reduced stresses. It is insufficient to proper shot peening treatment parameters design, allowing to obtain the required surface layer properties. Thus it is also insufficient to predict how parts will be work load. The numerical modeling and simulations do not have those restrictions, and allows to obtain the full knowledge about the all internal stress components.

In this paper the mixed explicit-implicit method of numerical simulation of shot peening process is proposed and presented. It allows to obtain the internal (plastic) stress components, leaving the elastic stresses.

1. PHYSICAL MODEL

The goal of this modeling process is to determinate the fields of all internal stress components after shot peening process. The following assumptions, concerning the object composed of workpiece surface layer and shot , were taken into account during model creation:

1. Both, workpiece surface layer and shot are treated as continuous media.
2. The workpiece surface layer is elastic/viscous-plastic body.

3. The shot is ideally rigid body.
4. Both, workpiece surface layer and shot are made from isotropic materials.
5. The three dimensional states of strain and stress were assumed.

2. MATHEMATICAL MODEL

State of stress can be described by symmetric, second-order tensor, with six different components. One may transform this tensor to six component vector:

$$\sigma = \left[\sigma_x\ \sigma_y\ \sigma_z\ \sigma_{xy}\ \sigma_{yz}\ \sigma_{xz}\right]^T, \tag{1}$$

where: σ_x, σ_y, σ_z are normal stress along the adequate axis, and σ_{xy}, σ_{yz}, σ_{xz} are shear stress along the adequate plane.
Also the strain state tensor may be formed to six component vector, in form analogical to the form of vector (1):

$$\varepsilon = \left[\varepsilon_x\ \varepsilon_y\ \varepsilon_z\ \varepsilon_{xy}\ \varepsilon_{yz}\ \varepsilon_{xz}\right]^T, \tag{2}$$

where: ε_x, ε_y, ε_z are normal strain along the adequate axis, and ε_{xy}, ε_{yz}, ε_{xz} are shear strain along the adequate plane.

The nonlinearity and high complexity, combined with lack of knowledge of boundary conditions in contact zone, required modern methods of shot peening modeling process. The equation which describes the motion of the object on a typical time step (fig. 1) in an updated Lagrange`s description has the following form:

$$[\mathbf{M}]\{\Delta\ddot{\mathbf{r}}\} + [\mathbf{C}_T]\{\Delta\dot{\mathbf{r}}\} + \left([\mathbf{K}_T] + [\Delta\mathbf{K}_T]\right)\{\Delta\mathbf{r}\} = \{\Delta\mathbf{R}\} + \{\Delta\mathbf{F}\} + \{\mathbf{R}\} + \{\mathbf{F}\}, \tag{3}$$

where:
- $[\mathbf{M}]$ – global mass matrix of the system at time t,
- $[\mathbf{C}_T]$ – global damping matrix of the system at time t,
- $[\mathbf{K}_T]$ – global stiffness matrix at time t,
- $[\Delta\mathbf{K}_T]$ – global matrix of the increment of the object`s stiffness on a step time Δt,
- $\{\mathbf{F}\}$ – global internal load vector of an system at time t,
- $\{\Delta\mathbf{F}\}$ – global increment vector of the systems internal loads on step time Δt,
- $\{\mathbf{R}\}$ – global external load vector of an system at time t,
- $\{\Delta\mathbf{R}\}$ – global increment vector of the systems external loads on step time Δt,
- $\{\Delta\mathbf{r}\}$ – global increment vector of the displacements of the system`s nodes on step time Δt,
- $\{\Delta\dot{\mathbf{r}}\}$ – global increment vector of the velocity of the system`s nodes on step time Δt,
- $\{\Delta\ddot{\mathbf{r}}\}$ – global increment vector of the accelerations of the system`s nodes on step time Δt.

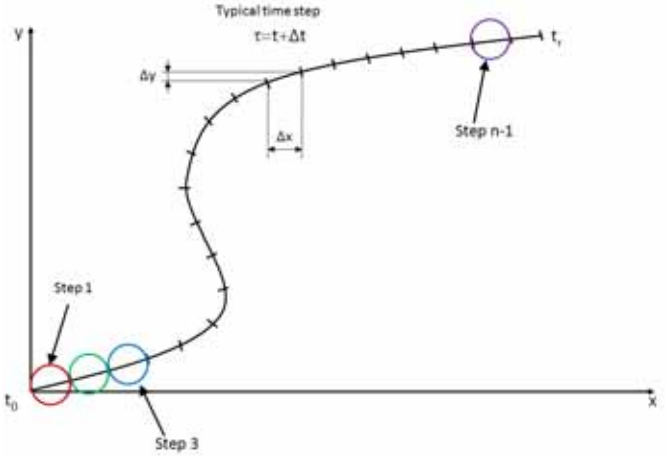

Fig. 1. Evolution of object motion
Source: own development.

Analytical solution of equation (3) is impossible, due to proportions of number of equation (N) and $5N$ unknowns of vectors: $\{\Delta\mathbf{r}\}$, $\{\Delta\dot{\mathbf{r}}\}$, $\{\Delta\ddot{\mathbf{r}}\}$, $\{\Delta\mathbf{F}\}$, $\{\Delta\mathbf{R}\}$, and N^2 unknowns in matrix $[\Delta\mathbf{K}_T]$. Only approximate solution is possible, for this purpose it is necessary to reduce the number of unknown variables occurring in equation (3). Using linearization:

$$[\mathbf{M}]\{{}_t^{\tau}\Delta\ddot{\mathbf{r}}\}+[\mathbf{C}_T]\{{}_t^{\tau}\Delta\dot{\mathbf{r}}\}+[{}_t^{t}\mathbf{K}_T]\{{}_t^{\tau}\Delta\mathbf{r}\}=\{{}_t^{t}\mathbf{F}\}+\{{}_t^{\tau}\Delta\mathbf{R}\}+\{{}_t^{t}\mathbf{R}\}, \tag{4}$$

and incremental decomposition:

$$\{{}_t^{\tau}\Delta\ddot{\mathbf{r}}\}=\{{}_t^{\tau}\ddot{\mathbf{r}}\}-\{{}_t^{t}\ddot{\mathbf{r}}\},\quad \{{}_t^{\tau}\Delta\dot{\mathbf{r}}\}=\{{}_t^{\tau}\dot{\mathbf{r}}\}-\{{}_t^{t}\dot{\mathbf{r}}\},\ \{{}_t^{\tau}\Delta\mathbf{R}\}=\{{}_t^{\tau}\mathbf{R}\}-\{{}_t^{t}\mathbf{R}\}, \tag{5}$$

equation (3) for typical time step can be transformed in to the form:

$$[\mathbf{M}]\{{}_t^{\tau}\Delta\ddot{\mathbf{r}}\}+[\mathbf{C}_T]\{{}_t^{\tau}\Delta\dot{\mathbf{r}}\}+[{}_t^{t}\mathbf{K}_T]\{{}_t^{\tau}\Delta\mathbf{r}\}=\{{}_t^{t}\mathbf{F}\}+\{{}_t^{\tau}\Delta\mathbf{R}\}+\{{}_t^{t}\mathbf{R}\}. \tag{6}$$

Next we can eliminate the expression:

$$\{{}_{t-\Delta t}^{\ t}\mathbf{F}_T\}=[{}_{t-\Delta t}^{t-\Delta t}\mathbf{K}_T]\{{}_{t-\Delta t}^{\ t}\Delta\mathbf{r}\}-\{{}_{t-\Delta t}^{t-\Delta t}\mathbf{F}_T\}, \tag{7}$$

thereby we obtain:

$$[\mathbf{M}]\{{}^t\ddot{\mathbf{r}}\}+[\mathbf{C}_T]\{{}^t\dot{\mathbf{r}}\}=\{{}^t\mathbf{R}\}+\{{}^t\mathbf{F}_T\}. \tag{8}$$

Next, according to explicit integration method, we can adopt differential approximation of displacements partial derivatives:

$$\{{}^t\dot{\mathbf{r}}\}=(2\Delta t)^{-1}(\{{}^{t+\Delta t}\mathbf{r}\}-\{{}^{t-\Delta t}\mathbf{r}\}), \tag{9}$$

$$\{{}^t\ddot{\mathbf{r}}\}=\Delta t^{-2}(\{{}^{t+\Delta t}\mathbf{r}\}-2\{{}^t\mathbf{r}\}+\{{}^{t-\Delta t}\mathbf{r}\}). \tag{10}$$

Finally determining effective mass matrix as:

$$[\widetilde{\mathbf{M}}]=(\Delta t)^{-2}[\mathbf{M}]+(2\Delta t)^{-1}[\mathbf{C}_T], \tag{11}$$

and effective loads vector as:

$$\{{}^t\widetilde{\mathbf{Q}}\}=\{{}^t\mathbf{R}\}+\{{}^t\mathbf{F}_T\}+2(\Delta t)^{-2}[\mathbf{M}]\{{}^t\mathbf{r}\}-\left((\Delta t)^{-2}[\mathbf{M}]-(2\Delta t)^{-1}[\mathbf{C}_T]\right)\{{}^{t-\Delta t}\mathbf{r}\}, \tag{12}$$

we obtain the equation (3) in form:

$$[\widetilde{\mathbf{M}}]\{{}^{t+\Delta t}\mathbf{r}\}=\{{}^t\widetilde{\mathbf{Q}}\}. \tag{13}$$

Therefore equation (13) is to be satisfied only in the selected time intervals, and not in the whole interval in question. This means that for each moment, one can look for the balance points of the system subject to the action of external, internal and dumping forces, while applying static analysis algorithms. The end of each time moment is simultaneously the beginning of next time step.

For dynamic part of simulations a Cowper-Symond`s elastic/viscous-plastic material model, which allows linear-isotropic (β=1), kinematic (β=0) or mixed (0<β<1) plastic strain hardening, was applied:

$$\sigma_{\mathrm{Y}}=(\mathrm{R_e}+\beta\cdot\mathrm{E_{tan}}\cdot\varphi_{\mathrm{i}}^{(\mathrm{p})})[1+(\dot{\varphi}_{\mathrm{i}}^{(\mathrm{p})}\cdot\mathrm{C}^{-1})]^{\mathrm{m}}, \tag{14}$$

where:

- β [-] – the parameter of plastic strain hardening,
- $\mathrm{R_e}$ [MPa] – the initial, static yield point,
- $\varphi_{\mathrm{i}}^{(\mathrm{p})}$[-] – the plastic true strain intensity,

– $\dot{\varphi}_{\mathrm{i}}^{(\mathrm{p})}\left[s^{-1}\right]$ – the intensity of plastic true strain rate,
– $C\left[s^{-1}\right]$ – the material parameter defining the effect of intensity of plastic strain rate,
– m=1/P – material constant defining the material sensitivity to the plastic strain rate,
– $E_{\tan}=\left(E_T\cdot E\right)\left(E-E_T\right)^{-1}$ – the material parameter depending on the modulus of plastic strain hardening $E_T=\partial\sigma_P\left(\partial\varphi_i^{(P)}\right)^{-1}$ and Young`s modulus E.

For static analysis the bilinear kinematic hardening material model (fig. 2) was applied.

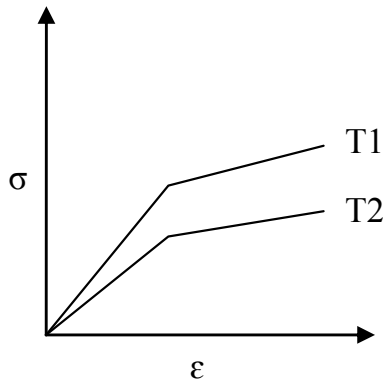

Fig. 2. Bilinear kinematic hardening material model

Source: ANSYS 12.1 help, 8.4 Modeling Material Nonlinearities.

3. NUMERICAL MODEL

The numerical simulations of shot peening process were made using the commercial software package for FEM analysis – ANSYS/LS-DYNA (for dynamic) and ANSYS Multi-physics (for static) . The three dimensional states of strain and stress have been taken into consideration. The shot diameter was 3mm, while its initial velocity was equal to 100 $m\cdot s^{-1}$. Single shot hit into the work surface was simulated. Both, the shot and the work surface were meshed with three-dimensional finite elements type SOLID164 for dynamic analysis, and SOLID185 for static one. Workpiece surface layer model consisted 486000 finite elements concentrated in contact zone, while shot was discredited with 60000 finite elements. The discrete numerical model with boundary conditions is shown in fig. 3. The material model for shot was modeled as ideal rigid St 170 cast steel. However the work surface was treated as elastic/viscous-plastic (for dynamic) or bilinear kinematic hardening (for static) body made from 50S2 spring steel. Material parameters value used in simulation is shown in table 1.

Tab. 1. Material constants used for simulation

Parameter	Dynamic simulation		Static simulation	SI Units
	Surface layer - 50S2 (elastic/viscous-plastic body)	Shot - St170 (rigid body)	Surface layer - 50S2 (bilinear kinematic hardening body)	
Density	7865	7800	7865	$kg \cdot m^{-3}$
Young`s Modulus	200	206	200	GPa
Poisson ratio	0,3	0,29	0,3	-
Elastic limit	1080	-	1080	MPa
Modulus of strain hardening	1280	-	1280	MPa
Strain hardening coefficient	1	-	-	-
Parameter (c)	40	-	-	-
Parameter (p)	5	-	-	s^{-1}
Critical strain	0.75	-	-	-

Source: Bartosik P., Szyc M., Kukiełka L.: *Analiza możliwości sterowania rozkładem naprężeń wynikowych w warstwie wierzchniej zęba kultywatora po kulowaniu w aspekcie wytrzymałości zmęczeniowej*. Inżynieria Rolnicza 9 (118)/2009, s. 7-14.

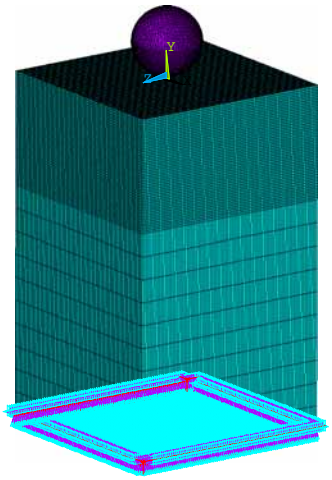

Fig. 3. Discrete numerical model

Source: ANSYS 12.1.

The numerical simulation were carried out in two stages. In first step the dynamic simulation was conducted, to produce the states of stress and strain in surface layer, caused by shot hit on to the surface of the object. Next the static analysis has allowed to relax the elastic stresses. Thereby only the plastic stresses remained in the surface layer of analyzed object.

4. RESULTS

Figure 4 shows the model velocity in the various stages of shot hit on to surface of the object. Figures 5-10 show the maps of the individual components of internal stress, from dynamic (with elastic stress) and static (after relaxation of elastic stress) analysis. Analogously figures 11 and 12 show the patterns of normal and shear stress into the material. The large fluctuation on figure 12 are related with low value of shear stresses occurring in surface layer (not exceeding ±2 MPa). Finally figure 13 presents relation of displacement of node located directly in the center of shot impact versus time of process.

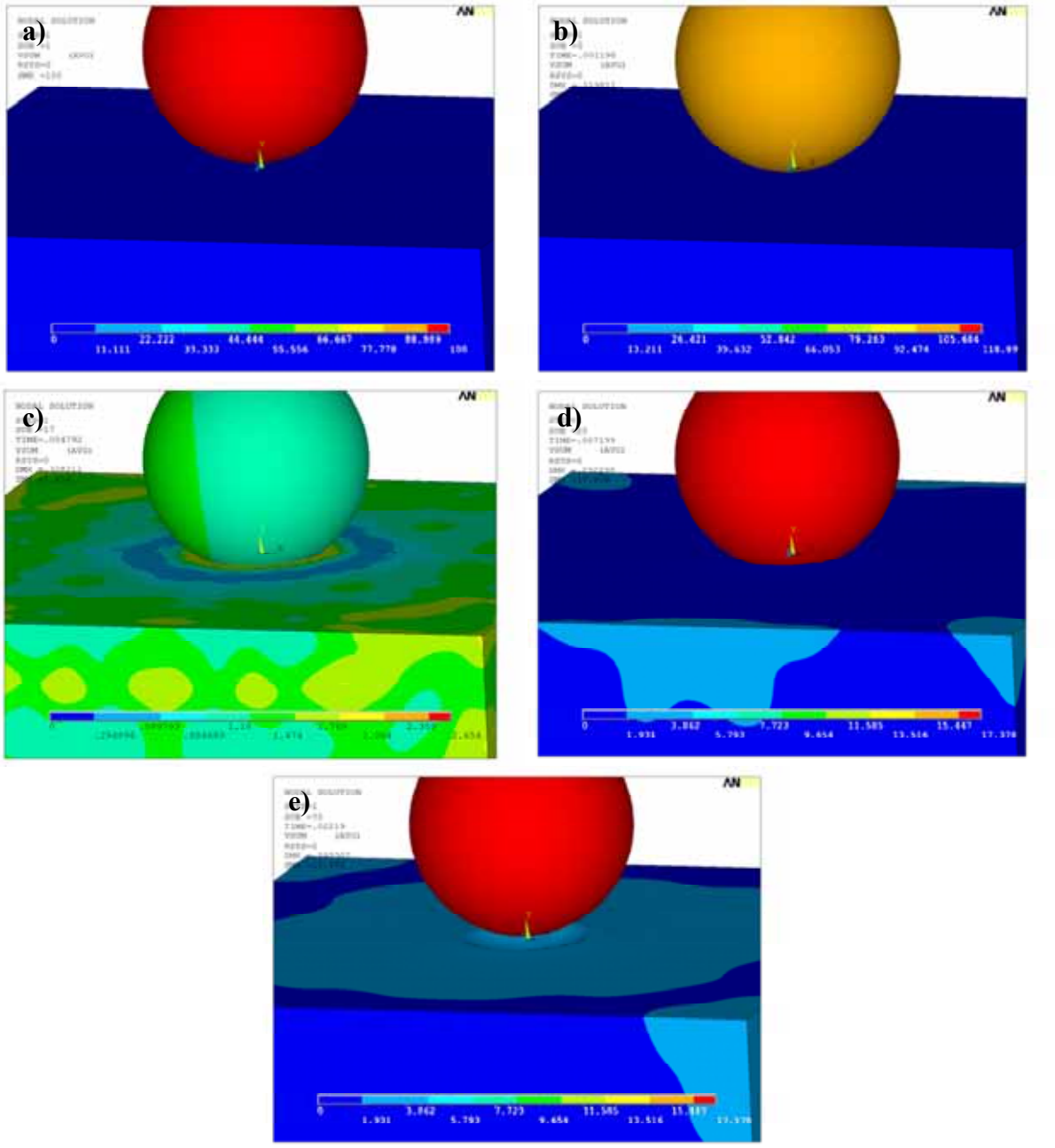

Fig. 4. Model velocity [m·s^{-1}] in the various stages of shot hit on to surface of the object: a) initial velocity, b) contact beginning, c) maximum penetration, d, e) reflection

Source: Own study in ANSYS 12.1.

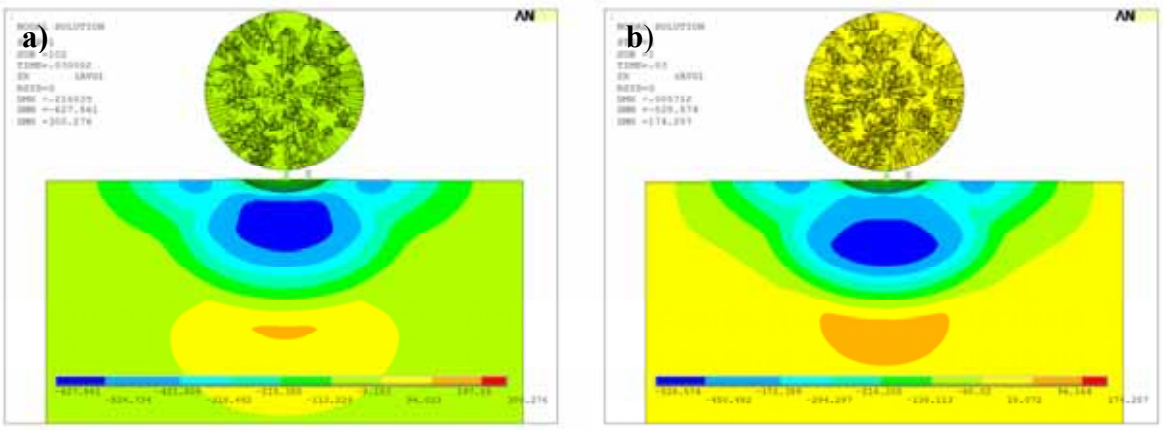

Fig. 5. Map of σ_x [MPa] normal stress: a) after dynamic analysis, b) after static analysis
Source: Own study in ANSYS 12.1.

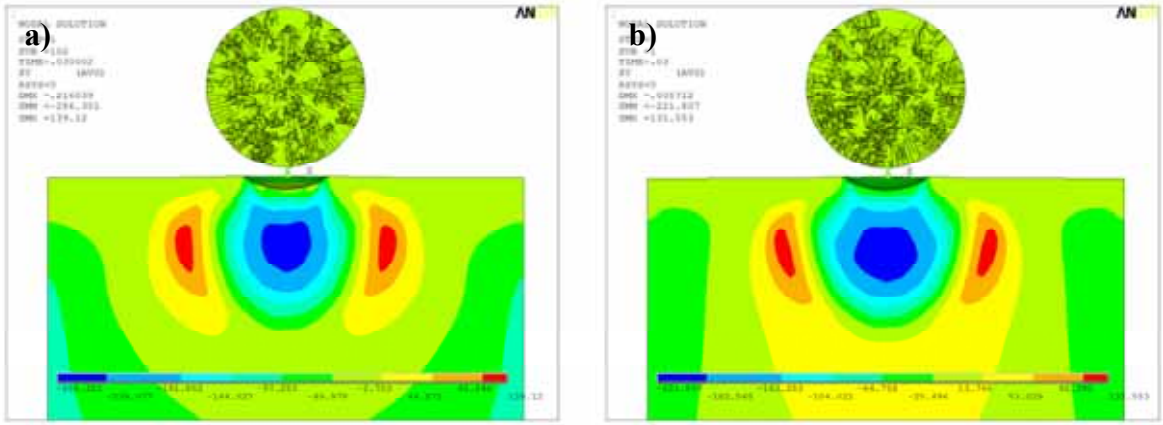

Fig. 6. Map of σ_y [MPa] normal stress: a) after dynamic analysis, b) after static analysis
Source: Own study in ANSYS 12.1.

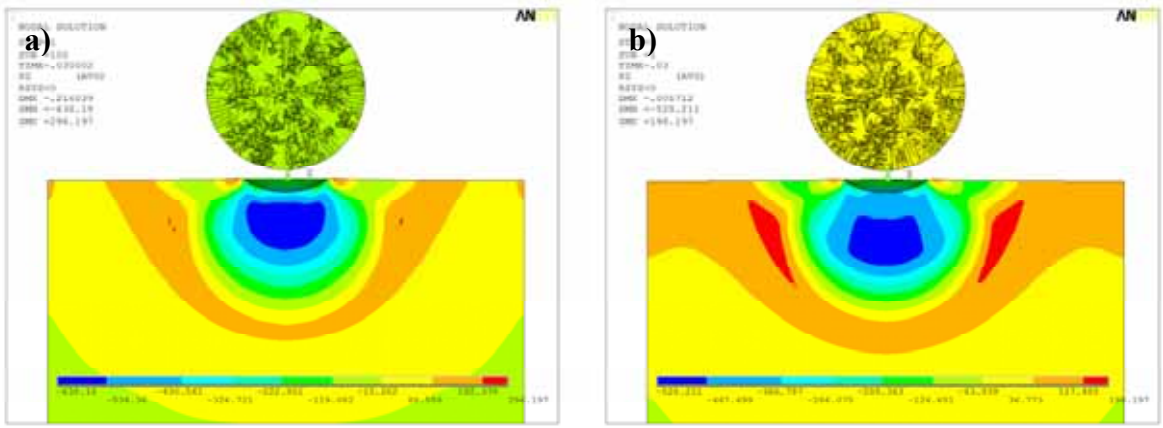

Fig. 7. Map of σ_z [MPa] normal stress: a) after dynamic analysis, b) after static analysis
Source: Own study in ANSYS 12.1.

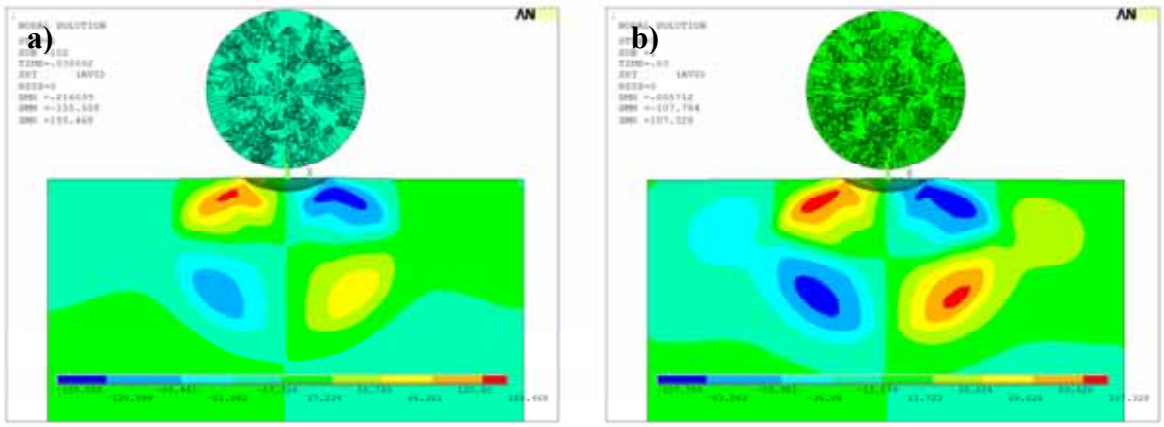

Fig. 8. Map of σ_{xy} [MPa] shear stress: a) after dynamic analysis, b) after static analysis
Source: Own study in ANSYS 12.1.

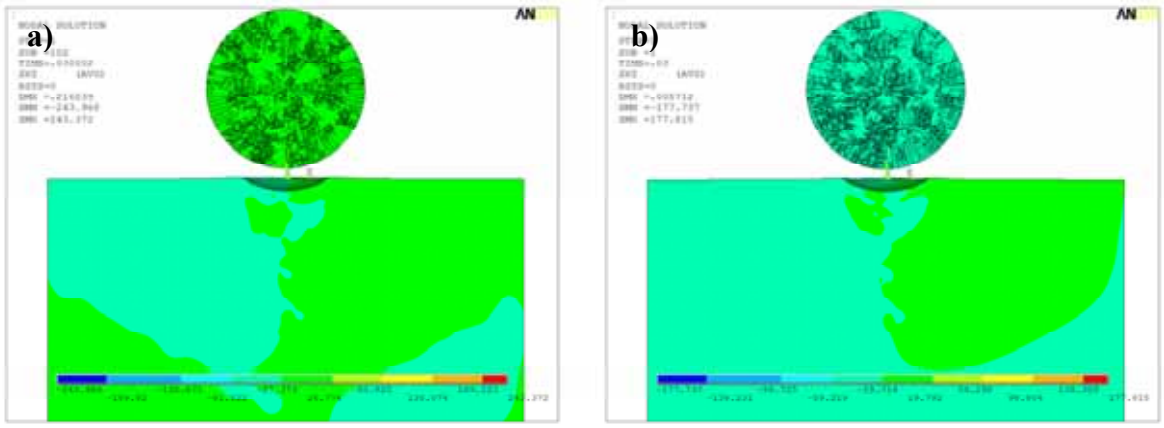

Fig. 9. Map of σ_{xz} [MPa] shear stress: a) after dynamic analysis, b) after static analysis
Source: Own study in ANSYS 12.1.

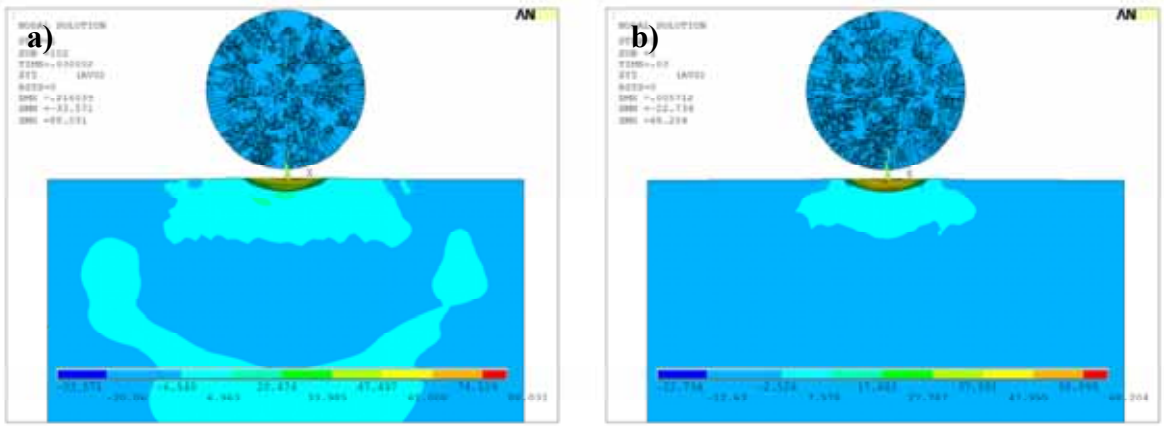

Fig. 10. Map of σ_{yz} [MPa] shear stress: a) after dynamic analysis, b) after static analysis
Source: Own study in ANSYS 12.1.

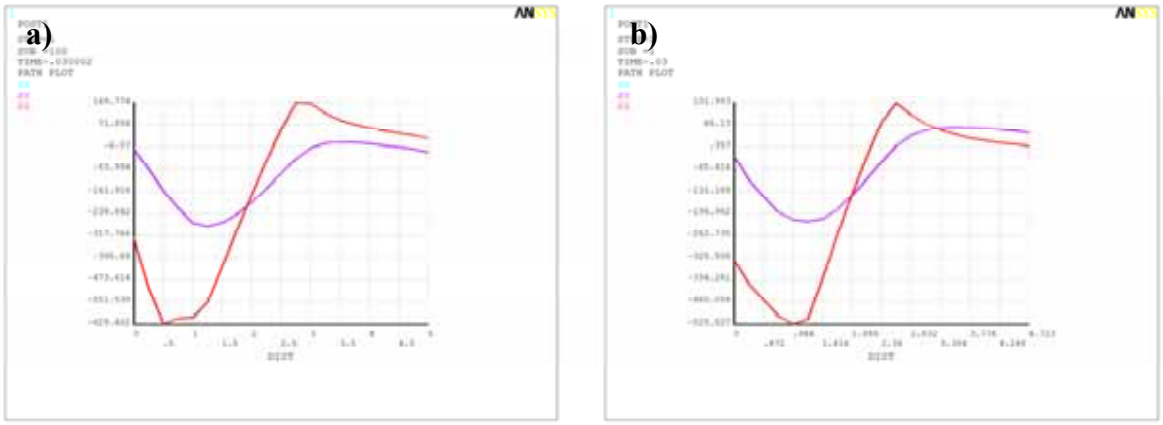

Fig. 11. Normal stress distribution [MPa]: a) after dynamic analysis, b) after static analysis

Source: Own study in ANSYS 12.1.

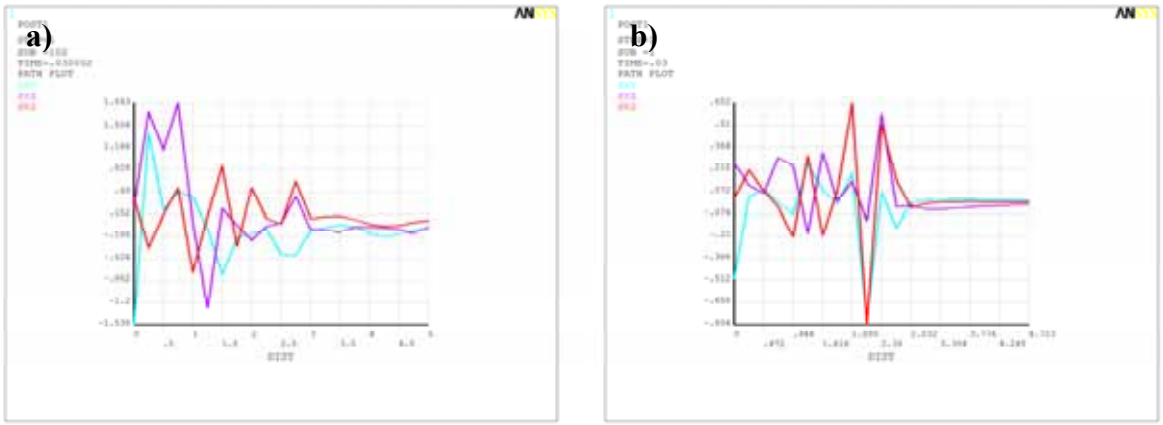

Fig. 12. Shear stress distribution [MPa]: a) after dynamic analysis, b) after static analysis

Source: Own study in ANSYS 12.1.

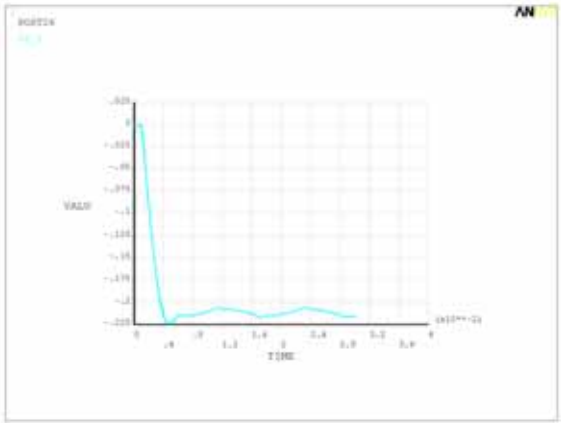

Fig. 13. Relation of displacement [mm] of node located directly in the center of shot impact versus time [s]

Source: Own study in ANSYS 12.1.

CONCLUSIONS

The elaborated applications in ANSYS/LS-DYNA and ANSYS Multiphysics environment allows to simulation many different physical phenomena (stress, strain, deformation, thrust, slip, adhesion etc.) occur during the shot peening process, especially provides determination of all components of internal stress. Through numerical simulations it is possible to predict the internal stress distribution without need to carry out expensive and time-consuming empirical experiments. Moreover knowledge about all tensor components value will allow in future to consciously control of shot peening process parameters in desired internal stress distribution generating aspect.

REFERENCES

1. Bartosik P., Szyc M., Kukiełka L.: *Analiza możliwości sterowania rozkładem naprężeń wynikowych w warstwie wierzchniej zęba kultywatora po kulowaniu w aspekcie wytrzymałości zmęczeniowej*, Inżynieria Rolnicza 2009, nr 9(118).
2. Kobayashi M., Matsui T., Murakami Y.: *Mechanism of creation of compressive residual stress by shot peening*, Int. J. Fatigue, 1998, Vol. 20.
3. Levers A., Prior A.: *Finite element analysis of shot peening*. Journal of Materials Processing Technology, 1998.
4. Majzoobi G.H., Azizi R., Alavi Nia A.: *A three-dimensional simulation of shot peening process using multiple shot impacts*. Journal of Materials Processing Technology, 2005.
5. Nakonieczny A.: *Effect of shot peening on fatigue life of machine elements*, Institute of Precision Mechanics, Warsaw, 1980.
6. Yu-Kui G., Mei Y., Jin-Kui L.: *An analysis of residual stress fields caused by shot peening*. Metallurgical And Materials Transactions, A Volume 33A, 2002.

PRZESTRZENNE MODELOWANIE I SYMULACJA NUMERYCZNA PROCESU KULOWANIA CZĘŚCI SILNIKÓW

Streszczenie

Praca dotyczy modelowania i symulacji komputerowej procesu kulowania. Autorzy zaproponowali i przedstawili łączoną dynamiczno-statyczną metodę wyznaczania naprężeń plastycznych. Zastosowano przyrostowy, uaktualniony opis Lagrange'a oraz adekwatne miary odkształceń i naprężeń. Przedstawiono modele fizyczny, matematyczny i numeryczny procesu dynamicznego nagniatania. Materiał przedmiotu nagniatanego traktowano jako ciało sprężysto/lepko-plastyczne z nieliniowym umocnieniem mieszanym, natomiast śrut jako ciało idealnie sztywne lub sprężyste. Przedstawiono przykładowe wyniki analiz numerycznych.

***Authors**:*

mgr inż. **Przemysław Bartosik** – Politechnika Koszalińska

prof. dr hab. inż. **Leon Kukiełka** – Politechnika Koszalińska